



From southern refugia to the northern range margin: genetic population structure of the common wall lizard, *Podarcis muralis*

Franz Gassert^{1*}, Ulrich Schulte², Martin Husemann³, Werner Ulrich⁴, Dennis Rödder⁵, Axel Hochkirch², Edmée Engel¹, Jobst Meyer⁶ and Jan Christian Habel⁷

¹Department of Vertebrate Biology, Natural History Museum Luxembourg, L-2160, Luxembourg, ²Department of Biogeography, Trier University, D-54296, Trier, Germany, ³Biology Department, Baylor University, Waco, TX, 76798, USA, ⁴Department of Animal Ecology, Nicolaus Copernicus University, PL-87100, Toruń, Poland, ⁵Zoologisches Forschungsmuseum Alexander Koenig, D-53113, Bonn, Germany, ⁶Department of Neurobehavioral Genetics, Trier University, D-54290, Trier, Germany, ⁷Department of Ecology and Ecosystem Management, Technische Universität München, D-85350, Freising-Weihenstephan, Germany

ABSTRACT

Aim Thermophilic species persisted in southern refugia during the cold phases of the Pleistocene, and expanded northwards during warming. These processes caused genetic imprints, such as a differentiation of genetic lineages and a loss of genetic diversity in the wake of (re)colonization. We used molecular markers and species distribution models (SDMs) to study the impact of range dynamics on the common wall lizard, *Podarcis muralis*, from southern refugia to the northern range margin.

Location Parts of the Western Palaearctic.

Methods We genotyped 10 polymorphic microsatellites in 282 individuals of *P. muralis* and sequenced the mitochondrial DNA (mtDNA) cytochrome *b* gene to study the genetic structure, divergence times and ancestral distributions. Furthermore, we generated SDMs for climate scenarios for 6 and 21 ka derived from two different global circulation models.

Results We detected two major mtDNA lineages – a western France clade (Pyrenees to Brittany), and an eastern France clade (southern France to Germany, Belgium and Luxembourg). This split was dated to *c.* 1.23 Ma. The latter clade was divided into two subclades, which diverged *c.* 0.38 Ma. Genetic diversity of microsatellites within each clade was nested and showed a significant loss of genetic diversity from south to north, a strong pattern of allele surfing across nearly all loci, and an increase in genetic differentiation towards the northern range margin. Results from SDMs suggest that southward range retraction during the late glacial period split the distribution into geographically distinct refugia.

Main conclusions The strong genetic differentiation mirrors the effects of long-term isolation of *P. muralis* in multiple refugia. Post-glacial recolonization of Northern Europe has taken place from two distinct refugia, most probably along river systems (Rhône, Rhine, Moselle) and along the Atlantic coastline, with subsequent nested elimination of genetic diversity and increasing genetic differentiation at the northern range margin.

Keywords

Climatic oscillations, Europe, genetic structure, leading edge, lizard phylogeography, microsatellites, post-glacial pathways, rear edge, refugia, species distribution models.

*Correspondence: Franz Gassert, Department of Vertebrate Biology, Natural History Museum Luxembourg, 25, rue Münster, L-2160 Luxembourg.
E-mail: franz.gassert@gmx.de

INTRODUCTION

Quaternary climatic oscillations caused severe range shifts in European biota (Sommer & Zachos, 2009). Thermophilic

species were widespread in Central Europe during the warmer interglacial periods, but retracted to southern refugia during the cold phases (Hewitt, 2000). Geographical separation and long-lasting persistence in these refugia caused

divergence of local populations and the evolution of genetic lineages or even speciation. As a result of post-glacial warming, these differentiated genetic lineages spread over large parts of Europe (Habel *et al.*, 2010). This northward (re)colonization was often accompanied by several genetic phenomena, such as the secondary contact of two or more genetic lineages along hybrid zones (Hewitt, 2000) and the stepwise loss of genetic diversity from south to north due to subsequent repeated founder effects at the colonization front (Hampe & Petit, 2005). High genetic diversity can often be detected in populations located in former refugia (i.e. at the rear edge; Gómez & Lunt, 2007), while populations at the leading edge of a species' distribution are mostly characterized by lower genetic diversity, caused by the stepwise loss of alleles (Hampe & Petit, 2005). Furthermore, populations at the leading edge of the expansion are also characterized by strong population fluctuations, high demographic stochasticity, and in consequence are often genetically strongly differentiated (Eckert *et al.*, 2008). This coherence has frequently been outlined in theory (e.g. Hampe & Petit, 2005), but few molecular studies have considered genetic structures over large parts of the geographical range of species – including both its rear and leading edges.

The common wall lizard, *Podarcis muralis* (Laurenti, 1768), has a sub-Mediterranean native range, extending to the Peloponnese and Calabria in the south, the Cantabrian mountains in the west, and north-western Anatolia in the east (Schulte, 2008). The north-western range margin runs along the French coast of the English Channel, across southern Belgium and the southernmost Netherlands towards south-western Germany (Gruschwitz & Böhme, 1986). Due to existing fossil records of the species *Podarcis praemuralis* Rauscher, 1992 from the upper Pliocene in Austria (Böttcher, 2007), it has been assumed that the species was distributed north of the Alps before the last glaciations. Previous studies have revealed genetic splits, indicating the existence of numerous evolutionary lineages and southern refugia on the Iberian Peninsula, in the Balkans and in particular on the Apennine Peninsula, where multiple refugia have been suggested (Gruschwitz & Böhme, 1986; Giovannotti *et al.*, 2010; Schulte *et al.*, 2012a,b).

We collected samples over the western part of the species' range, including populations from its northernmost range margin (Germany, Belgium and Luxembourg) and from the southern rear edge (southern France). Additionally, we sampled two populations from other potential refugia (central Italy and Croatia). Sequencing of the mitochondrial DNA (mtDNA) cytochrome *b* gene (*cyt b*) and genotyping of 10 polymorphic microsatellite loci were used to analyse the genetic structure in *P. muralis*. We used the mitochondrial data set and Bayesian approaches to estimate divergence times between lineages and to reconstruct their ancestral distributions. We then tested for nestedness of allele incidences, which should be found if the colonization followed a stepping-stone model with progressive loss of alleles. Furthermore, we generated species distribution models (SDMs)

using two different algorithms and a comprehensive set of species records, which were projected onto current and palaeoclimatic (6 and 21 ka) conditions in order to estimate the spatial distribution of *P. muralis* during the late glacial period. Based on these three approaches (mitochondrial gene phylogeny, microsatellite genotyping and SDM projections) we highlight processes at different temporal and spatial scales. In the following, we: (1) assess the location of potential glacial refugia; (2) reconstruct post-glacial recolonization pathways from south-west to north-west; (3) test for the loss of genetic diversity and the increase in genetic differentiation in the wake of post-glacial range expansion dynamics; and (4) analyse the effects of recent barriers and corridors at the landscape level.

MATERIALS AND METHODS

Sampling

We sampled 282 individuals at 20 sites for microsatellite analyses, and 50 individuals at 25 sites for the sequencing of *cyt b*. Specimens were collected between 2000 and 2010 by hand or by noosing. The sampling sites covered the major part of the western distribution range of the species (excluding the Iberian Peninsula) (Fig. 1, Table 1). Two further populations from the Balkan Peninsula (Pula, Croatia) and Italy (Alba Fucens, Abruzzo) were considered as outgroups. Lizards autotomized their tail tip after light pressure was exerted, and they were released immediately afterwards. The tail tip was stored in 96% pure ethanol until further processing.

DNA sequencing

DNA was extracted using the PeqGold Tissue DNA Mini Kit (Peqlab, Erlangen, Germany). We sequenced a fragment of *cyt b* using the following primers: (forward) Sicnt-L 5'-TTTGATCCCTGTTAGGCCTCTGTT-3' and (reverse) Melcb-H 3'-ATAATAAAAGGGGTGTTCTACTGGTTGGCC-5' (Deichsel & Schweiger, 2004), and a third additional internal primer (forward) L-15335 5'-AGGCACCTCCATAGTTCACC-3' (Podnar *et al.*, 2005). Sequencing was performed using the GenomeLab DTCS-Quick Start Kit (Beckman & Coulter, Brea, CA, USA). Sequencing reactions were run on a Genetic Analyzer CEQ 8000 (Beckman & Coulter). All DNA sequences were deposited in GenBank.

From each site, two individuals were sequenced, but only one sequence (25 in total) was used in subsequent analyses, as they were identical in all cases. We combined the sequences with 24 additional sequences of *P. muralis* obtained from GenBank (Carranza *et al.*, 2004; Busack *et al.*, 2005; Podnar *et al.*, 2007; Schulte *et al.*, 2008, 2012a,b; Giovannotti *et al.*, 2010). Additional sequences of *Podarcis siculus* (Rafinesque, 1810) (HQ154646, Podnar *et al.*, 2004), *Podarcis liolepis* (Boulenger, 1905) (JQ403296, Schulte *et al.*, 2012a) and *Podarcis melisellensis* (Braun, 1877) (AY185097,

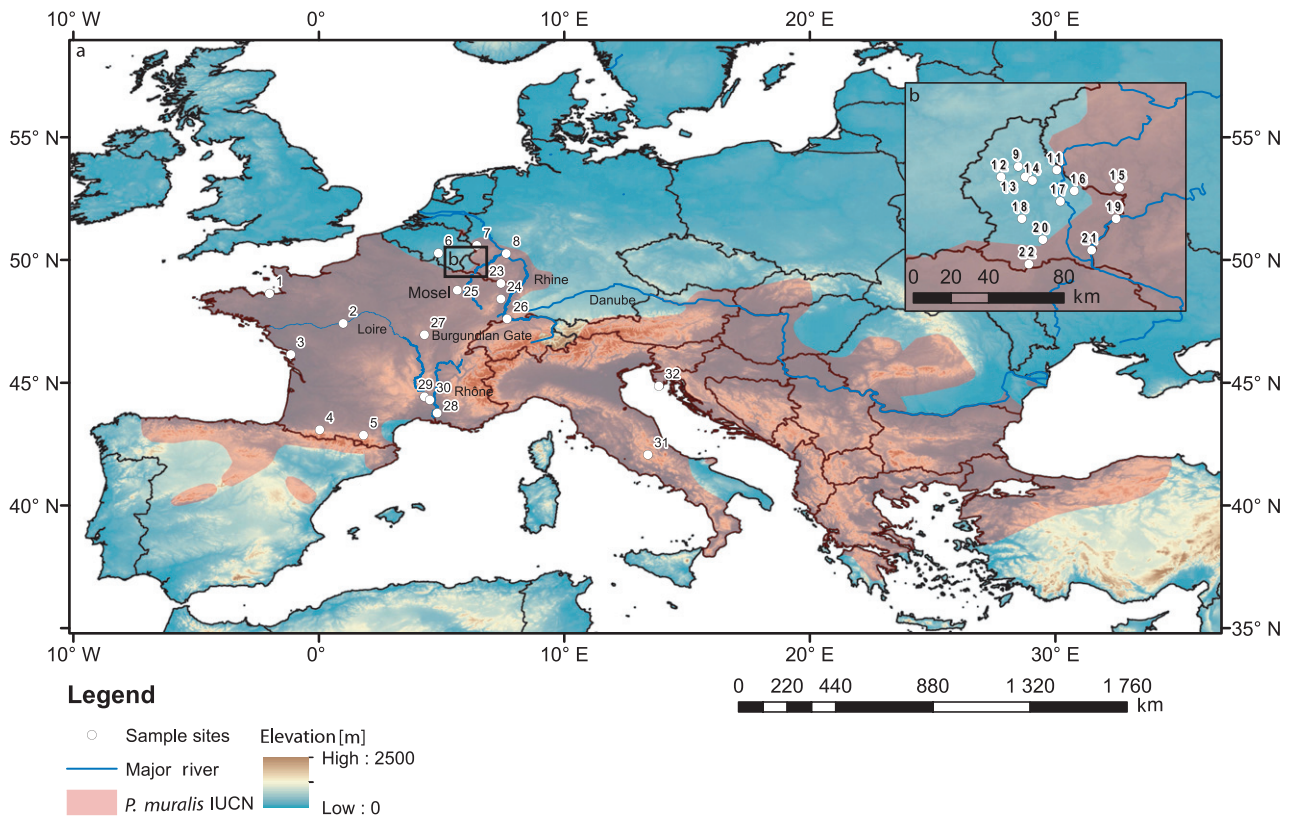


Figure 1 Locations of the sampling sites of *Podarcis muralis* in Europe. Site numbers match those given in Table 1. The Recent distribution of *P. muralis* (according to the IUCN Red List; Böhme *et al.*, 2009) is indicated by pink shading.

Podnar *et al.*, 2004) were included as outgroups (GenBank accession numbers are given in Appendix S1 in Supporting Information).

Sequences were aligned by eye and the alignment was trimmed to 1019 bp. Using MRMODELTEST (Nylander, 2004), the GTR+I+G model was determined to suit the data best, and was used for subsequent analysis in MRBAYES 3.1.2 (Huelsenbeck & Ronquist, 2001). Bayesian analysis was performed for three million generations, sampling every 1000 generations and discarding a burn-in of 500 samples. The results were checked in TRACER 1.5 for convergence of the chains (Rambaut & Drummond, 2009). The number of haplotypes and haplotype diversity were calculated in DNASP 5.0 (Librado & Rozas, 2009).

We performed a statistical dispersal–vicariance analysis as implemented in RASP 2.1 (Yu *et al.*, 2010, 2011) to reconstruct the ancestral distribution of each lineage; the combined output from two MRBAYES runs (6000 trees) served as the input file. We discarded a burn-in of 10%. The distributions of the main lineages were defined as geographical areas, whereas the outgroups' distributions were not considered. The maximum number of ancestral areas was set to four. Ten Markov chains were run with the default settings for 50,000 cycles, sampling every 100 generations and discarding a burn-in of 100 samples.

In addition, we performed a Bayesian analysis in BEAST 1.6.1 (Drummond & Rambaut, 2007) in order to estimate

divergence times. Because no fossils or reliable geographical calibration points were available, we used a strict clock with a fixed rate calibration. Substitution rates for the *cyt b* gene were obtained from publications estimating divergence times for other lineages of *Podarcis* (Harris *et al.*, 2002; Poulakakis *et al.*, 2003, 2005; Brown *et al.*, 2008). In our analyses, we employed a fixed rate of 1.75% per million years, representing the mean of the minimum (1.45%) and maximum (2.05%) estimates provided. The GTR+I+G model was chosen as the substitution model, and the Yule model was set as the tree prior. The Markov chain was run for 100 million generations sampling every 1000 generations. The resulting run parameters were checked for convergence in TRACER 1.5 (Rambaut & Drummond, 2009) and summarized with TREEANNOTATOR 1.6.1 (included in the BEAST package), discarding a burn-in of 10%. The tree was visualized using FIGTREE 1.3.1 (Rambaut, 2011).

Microsatellite genotyping

We genotyped 10 polymorphic microsatellite loci: A7, B3, B4, B6, B7, C8, C9, C24 (Nembrini & Oppliger, 2003), Lv-4-alpha and Lv-3-19 (Boudjemadi *et al.*, 1999). Amplification was performed in a MultiGene Gradient Thermal Cycler TC9600-G (Labnet, Edison, NJ, USA). For each PCR, we used a 25- μ L reaction mix containing 100 ng genomic DNA, 2 U *Taq* polymerase (Fermentas, St Leon-Rot, Germany),

Table 1 Sampling sites and parameters of genetic diversity given for *Podarcis muralis* in Europe. Given are geographical location (locality name and GPS coordinates), lineage assignment (according to mtDNA data), numbers of individuals used for microsatellites (n μ Sat) and mtDNA analysis (cytochrome b) as well as the following four parameters of genetic diversity calculated based on the analysis of 10 microsatellite loci: mean number of alleles (A), allelic richness (AR) (calculated based on a minimum of six individuals), expected heterozygosity (H_e) and observed heterozygosity (H_o). Abbreviations: W-France, western France clade; E-France, eastern France clade (including the Languedoc subclade for the population St-Martin); Tuscany, Tuscany clade; Marche, Marche clade; F, France; B, Belgium; D, Germany; L, Luxembourg; I, Italy; HR, Croatia. Population numbers match those given in Fig. 1.

Locality-PopID	GPS	Date of sampling	Clade	n μ Sat	n cyt b	A	AR	H_o (%)	H_e (%)
F-St Malo-1	48°38' N; 2°01' W	VII-2010	W-France	0	1	–	–	–	–
F-Amboise-2	47°25' N; 0°59' E	VII-2010	W-France	9	1	6.10	5.17	63.3	74.4
F-La Rochelle-3	46°09' N; 1°09' W	VII-2010	W-France	8	1	4.60	4.70	64.8	64.8
F-Lourdes-4	43°05' N; 0°02' E	VI-2009	W-France	6	1	5.40	5.40	60.0	75.5
F-Montségur-5	42°52' N; 1°49' E	VI-2009	W-France	13	1	7.00	5.10	68.4	69.1
B-Anhée-6	50°17' N; 4°52' E	VI-2003	E-France	18	1	3.10	2.67	50.7	42.5
D-Urft-7	50°36' N; 6°26' E	V-2003	E-France	10	1	4.60	3.89	50.0	64.5
D-Braubach-8	50°16' N; 7°38' E	VI-2008	E-France	0	1	–	–	–	–
L-Kautenbach-9	49°57' N; 6°01' E	VII-2009	E-France	15	1	5.80	4.41	58.0	67.5
L-Willerwilz-10	49°57' N; 5°55' E	VII-2009	E-France	0	1	–	–	–	–
L-Vianden-11	49°56' N; 6°12' E	VII-2009	E-France	0	1	–	–	–	–
L-Esch-sur-Sûre-12	49°54' N; 5°56' E	VII-2009	E-France	12	1	4.90	3.93	55.0	57.1
L-Burscheid-13	49°54' N; 6°03' E	VII-2009	E-France	0	1	–	–	–	–
L-Michelau-14	49°53' N; 6°05' E	VII-2009	E-France	9	0	4.40	3.91	64.4	62.5
L-Wark valley-15	49°51' N; 6°30' E	V-2007	E-France	28	1	4.70	3.44	57.9	53.6
L-Beaufort-16	49°50' N; 6°17' E	VIII-2009	E-France	0	1	–	–	–	–
L-Larochette-17	49°47' N; 6°13' E	VII-2009	E-France	0	1	–	–	–	–
L-Ansembourg-18	49°42' N; 6°02' E	VI-2008	E-France	10	1	2.80	2.63	60.0	42.0
L-Wasserbillig-19	49°42' N; 6°29' E	VII-2009	E-France	11	1	4.90	4.16	69.1	69.2
L-Lux.-city-20	49°36' N; 6°08' E	V-2007	E-France	18	1	4.90	3.88	63.9	56.3
L-Remich-21	49°33' N; 6°22' E	VIII-2009	E-France	30	1	6.40	4.12	63.0	65.9
L-Dudelange-22	49°29' N; 6°04' E	VII-2009	E-France	9	1	3.10	2.96	60.5	53.0
F-Bitche-23	49°03' N; 7°25' E	VII-2003	E-France	19	1	6.30	4.82	61.6	75.7
F-Mont St Odily-24	48°25' N; 7°25' E	VII-2009	E-France	20	1	5.50	3.89	50.0	61.8
F-Euville-25	48°46' N; 5°38' E	VII-2009	E-France	0	1	–	–	–	–
D-Lörrach-26	47°36' N; 7°40' E	VII-2008	E-France	0	1	–	–	–	–
F-Autun-27	46°57' N; 4°18' E	VII-2008	E-France	0	1	–	–	–	–
F-St Remy-28	43°46' N; 4°49' E	V-2003	E-France	0	1	–	–	–	–
F-Labeaume-29	44°26' N; 4°18' E	VII-2008	E-France	0	1	–	–	–	–
F-St-Martin-30	44°18' N; 4°31' E	VI-2004	E-France	16	1	9.80	6.63	78.7	86.2
I-Alba Fucens-31	42°04' N; 13°24' E	VI-2003	Tuscany	12	1	10.50	7.44	75.8	89.4
HR-Pula-32	44°52' N; 13°51' E	VI-2004	Marche	9	1	5.80	5.05	72.2	74.1

0.2 mM dNTPs, 1.5 mM MgCl₂ buffer, and 2.0 μ M of each primer. The PCR conditions were adjusted according to the locus-specific annealing temperatures, which varied between 53 °C and 60 °C (see references above). For genotyping, we multiplexed the following microsatellites: B3 with B6; A7 with C8; C9 with C24; B7 with B4; and Lv4-alpha with Lv-3-19. Fragments were visualized on an automated DNA sequencer (CEQ 8000; Beckman & Coulter, Fullerton, CA, USA). Fragment lengths were determined using CEQ 8000 Genetic Analysis System version 9.0.25 (Beckman & Coulter).

Population genetic analyses

Distortion of our microsatellite data through stutter bands, large-allele dropouts or null alleles (Selkoe & Toonen, 2006) were analysed with MICRO-CHECKER 2.2.3 (van Oosterhout *et al.*, 2004). Tests of Hardy–Weinberg equilibrium (HWE) and linkage disequilibrium were performed with ARLEQUIN 3.1 (Excoffier *et al.*, 2005).

Mean numbers of alleles, allelic richness and locus-specific allele frequencies were calculated in FSTAT 2.9.3.2 (Goudet, 1995). Hierarchical analyses of molecular variance (AMOVAs) and observed and expected levels of heterozygosity were calculated in ARLEQUIN 3.1 (Excoffier *et al.*, 2005). AMOVAs were carried out using the microsatellite-specific R -statistics. AMOVAs included three hierarchical levels of molecular variance – among regions (defined groups, i.e. mtDNA lineages; R_{CT}), among populations within groups (R_{SC}), and within populations.

Two assignment methods were chosen to classify individuals based on multiple nuclear loci. The first method is implemented in the program STRUCTURE 2.3.3 (Pritchard *et al.*, 2000) and is used to infer the most probable number of genetic clusters (K) using the admixture model. To define the most probable value of K , we used the ad hoc criteria $L(K)$ proposed by Pritchard *et al.* (2000) and ΔK by Evanno *et al.* (2005), ignoring the high ΔK value for $K = 2$ as

suggested by Hausdorf & Hennig (2010). STRUCTURAMA 2.0 was used to estimate the number of discrete genetic clusters (Huelsenbeck & Andolfatto, 2007; Huelsenbeck *et al.*, 2011). Multiple analyses were run to explore whether the results remained consistent. For both approaches, 10 runs were performed for each value of K , varying from 1 to 20, with burn-in and simulation length of 150,000 and 500,000 steps, respectively.

As a third approach to detect the correct genetic clustering of populations, we used the GENELAND 4.0.2 package (Guillot *et al.*, 2005) for R 2.15.1 (R Development Core Team, 2012). We used the correlated allele frequency model and performed 10 independent runs for 1–20 populations with 500,000 iterations, a thinning of 500 and a burn-in of 200. For the 13 populations at the northern range margin, we performed a separate GENELAND analysis with identical conditions, but additionally we performed the analysis with uncorrelated allele frequencies, as otherwise the most probable K was close to its maximum value ($K = 12$).

Tests for the significance of a correlation between geographical and pairwise genetic distance were performed [using the ratio $R_{ST}/(1-R_{ST})$ as a function of the distances between populations]. Pairwise genetic distances among populations were divided by the geographical distance among the respective populations analysed; the resulting matrix of relative genetic distances was correlated against latitude. Mantel tests as implemented in the program ARLEQUIN were used to check for 'isolation by distance'.

Nestedness analyses

To study patterns of *cyt b* allele incidences among our 20 sites, we constructed presence–absence matrices with alleles in rows and sites in columns (Habel *et al.*, 2013). We assessed the degree of nestedness along the presumed south to north colonization trajectory with the incidence-based NODF metric (nestedness by overlap and decreasing fill; Almeida-Neto *et al.*, 2008), which measures the matrix-wide degree of ordered decline in allele incidence along a pre-defined environmental or diversity gradient (Habel *et al.*, 2013). We used the nestedness contribution (Δ NODF, the difference in the degree of nestedness with and without a focal population; Saavedra *et al.*, 2011) to infer the importance of each population to the overall degree of nestedness.

Furthermore, we assessed patterns of allele co-occurrence using the common C -score metric (Stone & Roberts, 1992; Ulrich & Gotelli, 2013). High values of the C -score point to a segregated pattern of allele co-occurrence within populations. To assess the spatial turnover of alleles, we sorted rows and columns according to the first axis of the correspondence analysis and linked the order of sites and total numbers of alleles per site to the latitude and longitude (Ulrich & Gotelli, 2013). We quantified the spatial turnover of alleles by the squared coefficient of correlation R^2 between the row and column numbers of the ordinated matrix (Ulrich & Gotelli, 2013).

To test for statistical significance, we used a null-model approach (Gotelli & Ulrich, 2012) and compared the observed metrics with the distribution of metrics obtained from 200 randomized matrices. Because there is no a priori reason that constrains potential incidences of alleles across the sample sites, apart from selection pressure and bottleneck effects, we used the equiprobable null model *ee*, which controls only for the total number of alleles across all sample sites but does not fix the total numbers of incidences for certain alleles among sites or allele richness within sites (Gotelli, 2000). All calculations were performed using the software NODF (Almeida-Neto & Ulrich, 2011) and TURNOVER (Ulrich & Gotelli, 2013).

Species distribution models

For SDM development, we compiled species records from the Global Biodiversity Information Facility (GBIF, <http://www.gbif.org/>), HerpNet (<http://www.herpNet.org/>) and distribution information for common wall lizards within Natura 2000 sites provided by the European Environment Agency (<http://www.eea.europa.eu/data-and-maps/data/natura-2000-eunis-database>), in addition to our own field records. Species records were only considered when matching the resolution of the environmental predictors (see below), resulting in 3052 unique records. In order to minimize potential negative effects caused by varying sampling intensities across Europe, we thinned the total set using a spatial filter, leaving 500 randomly selected records with an equal density across the species' range (Schulte, 2008).

Climatic information for current conditions with a spatial resolution of 2.5 arc-minutes was obtained from the WorldClim database (<http://www.worldclim.org/>; Hijmans *et al.*, 2005) comprising a total of 19 bioclimatic variables (Beaumont *et al.*, 2005). As highly intercorrelated variables might negatively affect SDM performance (Heikkinen *et al.*, 2006), we tested for multicollinearity using confidence of determination and retained only those variables with $R^2 < 0.75$. The final set of predictors comprised: mean diurnal temperature range (BIO2); temperature seasonality (BIO4); annual temperature range (BIO7); mean temperature of the wettest quarter (BIO8); mean temperature of the warmest quarter (BIO10); mean temperature of the coldest quarter (BIO11); precipitation seasonality (BIO15); precipitation of the driest quarter (BIO17); precipitation of the warmest quarter (BIO18); and precipitation of the coldest quarter (BIO19).

For palaeoclimatic reconstructions, we down-scaled two palaeoclimatic scenarios simulating potential climatic conditions for 6 ka obtained from the PMIP2 Project [Community Climate System Model (CCSM), Otto-Bliessner *et al.* (2006); Model for Interdisciplinary Research on Climate (MIROC), Hasumi & Emori (2004); available through <http://pmip2.lscce.ipsl.fr/>; Braconnot *et al.* (2007)] to a spatial resolution of 2.5 arc-minutes, using the delta method described by Peterson & Nyári (2008). Data simulating palaeoclimatic

conditions for 21 ka derived from the same models were obtained from the WorldClim database, which were down-scaled to a resolution of 2.5 arc-minutes with the same method.

For SDM development, we used the algorithms MAXENT 2.0 (Phillips *et al.*, 2006; Phillips & Dudík, 2008; Elith *et al.*, 2011) and BIOCLIM 3.2 (Busby, 1991). MAXENT was run using the default settings and the logistic output format. As the environmental background, we defined an area enclosed by a circular buffer of 500 km enclosing all species records. Although several studies have highlighted that MAXENT might frequently outperform other SDM techniques (Elith *et al.*, 2006), we additionally employed BIOCLIM as a simpler environmental envelope technique because it allows a more intuitive interpretation of the results. To test the predictive performance of the models, we used a bootstrap approach and computed area under the receiver operating characteristic curve (AUC) scores (Swets, 1988). Therefore, the species records were divided into 70% used for model training and 30% for model testing. This procedure was repeated 10 times and the average prediction per grid cell was used to create the final maps.

Areas used for model training that exhibited non-analogous climatic conditions in the past to those currently present in the environmental background were identified using multivariate environmental similarity surfaces (MESS; Elith *et al.*, 2010) because extrapolation into these areas may be less certain.

RESULTS

Phylogenetic reconstruction using mtDNA sequences

We sequenced a total of 31 individuals from 31 geographical localities. The complete alignment contained 1019 sites, 140 of which were variable. A total of 28 haplotypes were found (including outgroups), resulting in a haplotype diversity of 0.867. Within *P. muralis*, the number of haplotypes was 25, with a haplotype diversity of 0.850; the nucleotide diversity (π) was 0.031, and the average number of nucleotide differences among localities (e.g. individuals) (k) was 13.94.

We identified two distinct genetic lineages in the western part of the range of *P. muralis*, both supported by high posterior probabilities (Fig. 2). The first group contains individuals from Luxembourg, Germany, Belgium and France (the 'eastern France clade'). This group can be further subdivided into two subclades: the eastern France main clade and the Languedoc subclade. The 'western France clade' was well supported and consisted of specimens from northern Spain, the Pyrenees and western France. These two French lineages had a weakly supported sister-group relationship (posterior probability, PP: 0.61). The next related clades were the southern Alps clade and the central Balkans clade. Specimens from Italy and Croatia belonged to two different genetic lineages, the Tuscany clade and the Marche clade, respectively. These clades are closely related to other Italian lineages. For

the eastern France clade, π was 0.0042 and k was 3.17, with 11 haplotypes, while for the western France clade, π was 0.0073 and k was 5.5, with five different haplotypes, reflecting the larger sample size for the eastern France clade ($n = 27$) than for the western France clade ($n = 5$).

Dating yielded robust results with relatively small highest posterior density (HPD) intervals (Fig. 3). According to this analysis, *P. muralis* split from *P. liolepis* c. 6 Ma. The diversification within *P. muralis* took place during the Pleistocene: the first split into two major clades occurred c. 2 Ma (France/Balkans versus Italy). The first of these clades splits into two lineages (1.44 Ma), one containing the southern Alps and central Balkans clade (split at 1.14 Ma) and the other one containing the western and eastern France clade (split at 1.23 Ma). The split between the eastern France main clade and the Languedoc clade occurred c. 0.38 Ma. The second major lineage (Italy) contains five clades, which split off sequentially: Calabria at 1.87 Ma; Tuscany at 1.19 Ma; Romagna at 1.05 Ma; and the final split between Venetia and Marche at 0.84 Ma (see Fig. 3).

The analysis in RASP indicated that dispersal had more influence on lineage diversification than vicariance (27 events compared to 12), and that the ancestral species was distributed in Calabria and dispersed from there to the Alps and Romagna ($P = 0.0166$). For all subsequent nodes, dispersal was the more likely explanation (see Appendix S2).

Population genetic structure based on microsatellite analyses

No linkage disequilibrium was observed for any pair of loci after Bonferroni correction. Significant deviations from Hardy–Weinberg equilibrium (due to the presence of null alleles) were detected in the following microsatellite loci in the following populations: C24: F-Montségur, L-Kautenbach and I-Alba Fucens; B4: D-Urft; B3: F-Bitche and F-Mont St Odily; B6: F-Mont St Odily.

Allelic richness was highest in southern populations (particularly I-Alba Fucens-31 and F-Saint-Martin-30) and lowest in the north (particularly L-Ansembourg-18, B-Anhée-6 and L-Dudelange-22). Similarly, heterozygosity values and the mean number of alleles (A) decreased from south to north (Table 1).

Nestedness analyses detected a significant decrease in genetic diversity from the rear edge to the northern range margin in both clades. In the western France clade, six loci were significantly nested when the study sites were ordered along the latitudinal gradient (Table 2). In the eastern France clade, all NODF standardized effect sizes (SES) scores were positive and nine were statistically significant at the 5% error level (two-tailed test; Table 2). Nestedness scores along the latitudinal gradient were stronger than the scores obtained from an ordering of the matrices according to row and column totals of incidence and richness, and were always higher than those obtained from different orderings of sites (not shown). In line with these findings, four loci showed a

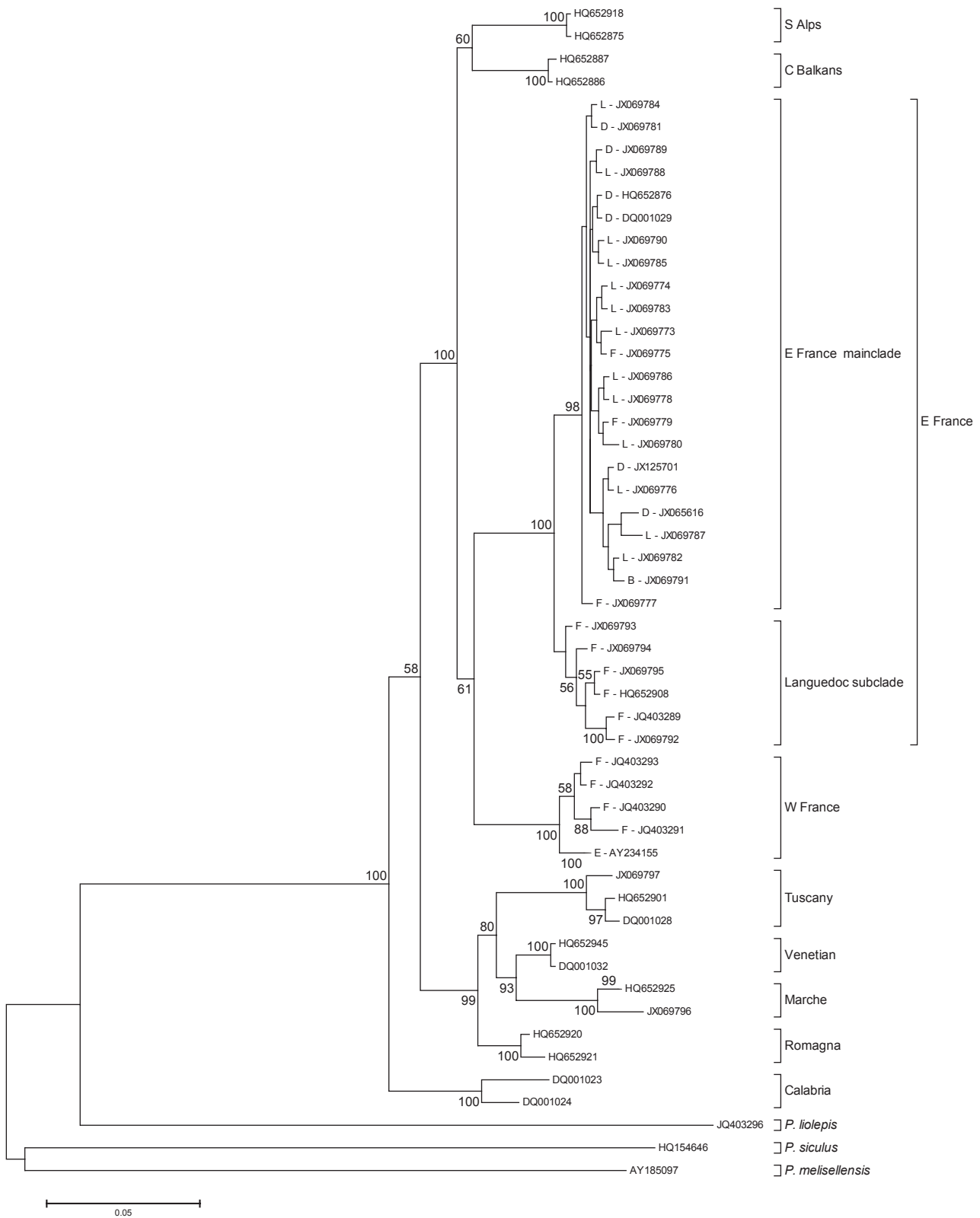


Figure 2 Bayesian consensus tree (50% majority rule) for the mitochondrial cytochrome *b* gene for *Podarcis muralis* [3 million Markov chain Monte Carlo (MCMC) generations, sampling frequency: 1000 generations, burn-in = 500]. Numbers are posterior probabilities. For the study area (western part of the range) the GenBank numbers are preceded by country abbreviations (L, Luxembourg; D, Germany; E, Spain; F, France). Other abbreviations: S = southern, C = central, E = eastern, W = western.

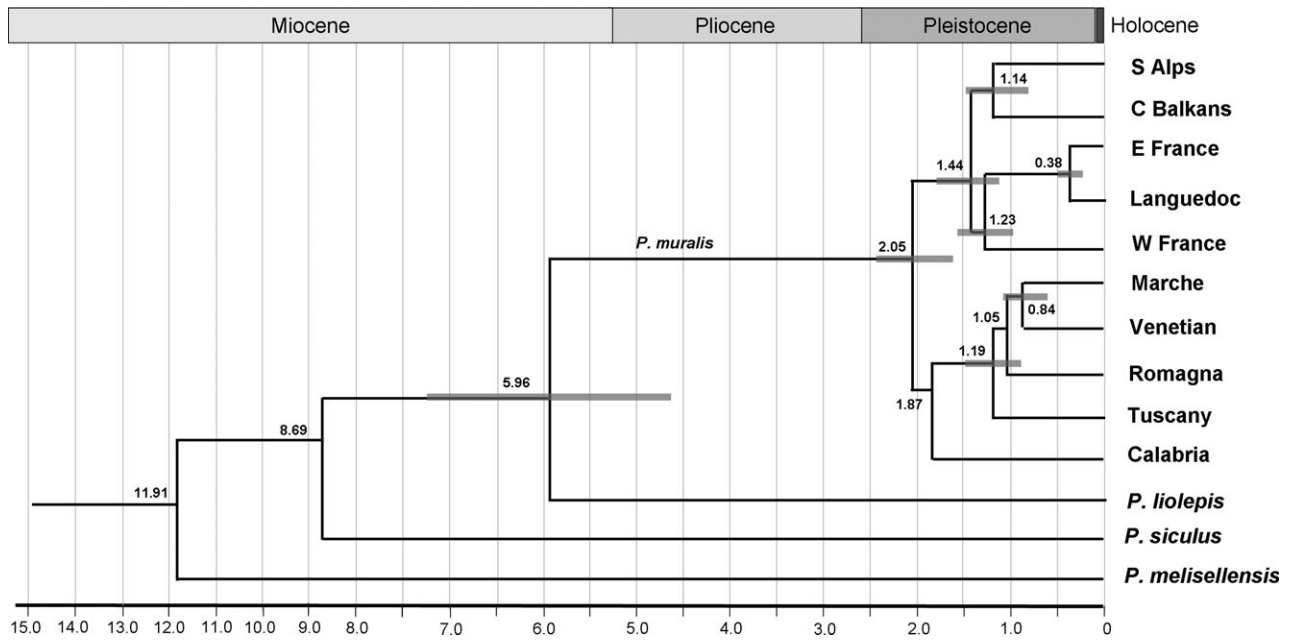


Figure 3 Divergence time estimates for each of the lineages of *Podarcis muralis* in Europe generated with BEAST using a fixed rate of 1.75% per Myr; numbers on nodes represent age estimates (Ma); grey bars indicate the 95% highest posterior densities (HPDs).

Table 2 Numbers of loci and standardized effect sizes (SES) of three presence–absence metrics of allele co-occurrence of the 10 polymorphic microsatellites studied at 4 sites of the western lineage and 14 sites at the eastern lineage of *Podarcis muralis* in Europe. SES scores of the *ee* null model distributions were approximately normal (not shown) and thus scores below -2 and above 2 point to statistical significance at the two-tailed 5% error level. High SES scores point to significant nestedness (NODF), spatial segregation of alleles (*C*-score), and spatial turnover (R^2).

	Locus									
Western lineage	B3	B6	B4	B7	C24	C9	A7	C8	Lv-3-19	Lv-4-alpha
Number	51	33	16	24	25	22	26	20	18	19
Metric	Matrix sorted according to latitude and allele incidences									
NODF	3.24	1.74	-0.02	3.64	2.67	0.89	3.64	4.49	2.81	1.88
Metric	Matrix sorted according to allele numbers and allele incidences									
NODF	-0.43	-0.26	-1.24	1.46	1.14	-2.72	1.05	1.52	0.31	-1.09
Metric	Matrix sorted according to the first correspondence axis									
R^2	0.32	-1.03	0.26	-0.85	-3.75	-0.56	-2.34	-1.58	-3.54	-1.94
<i>C</i> -score	0.03	-0.45	0.11	-1.09	-3.99	-1.85	-2.91	-0.85	-3.49	-2.13
	Locus									
Eastern lineage	B3	B6	B4	B7	C24	C9	A7	C8	Lv-3-19	Lv-4-alpha
Number	51	33	16	24	25	22	26	20	18	19
Metric	Matrix sorted according to latitude and allele incidences									
NODF	5.42	1.93	8.82	4.76	4.86	4.92	2.15	5.18	3.03	5.47
Metric	Matrix sorted according to allele numbers and allele incidences									
NODF	1.12	-0.81	12.79	1.92	2.56	6.00	1.85	7.78	2.14	4.52
Metric	Matrix sorted according to the first correspondence axis									
R^2	-2.54	-7.30	-2.82	-1.15	-4.37	-7.99	-6.73	-10.21	-7.47	-5.17
<i>C</i> -score	-9.55	-12.20	-12.15	-5.65	-9.86	-13.63	-14.54	-12.62	-8.83	-10.17

significant aggregated pattern of species co-occurrences and a lack of significant allele turnover among sites (Table 2). Patterns of allele co-occurrence for all loci were significantly aggregated with no indication of allele turnover (Table 2).

We also observed a significant decrease (Pearson’s $r = -0.59, P < 0.0001$) in the nestedness contribution of sites along this gradient. Partial correlation analysis to tease apart the influence of gradient and allele richness on nestedness con-

tribution confirmed this result and pointed to a higher influence of south-eastern European sites on the nested pattern of allele richness (partial correlation $r = -0.45$, $P < 0.0001$).

STRUCTURE revealed the highest ΔK for $K = 8$ (Appendix S3): (1) Italy and Croatia (populations 31, 32); (2) Alsace-Lorraine (23–24); (3) south-western Luxembourg (19, 21, 22); (4) Wark valley (15); (5) central Luxembourg (9, 14, 20); (6) Belgium and Germany (6, 7); (7) western France (2–5); and (8) eastern Luxembourg (12, 18). Individuals from the population St Martin (30) showed an admixed genetic architecture, consisting of genotypes from the populations of the south (Italy/Croatia) and the adjacent northern populations (Alsace-Lorraine). The population Amboise clustered within the western France clade, but also showed genetic affinities with eastern France populations (Fig. 4). STRUCTURAMA suggested $K = 10$ as the most probable number of genetic clusters (Appendix S3).

The most probable number of populations obtained from the GENELAND analysis using all populations analysed was $K = 14$. In this analysis, few populations were clustered together: (1) northern Luxembourg (9–15); (2) south-western Luxembourg (20, 21); (3) Alsace-Lorraine (23, 24); and (4) western France (3–5). A separate run for the northern range margin revealed $K = 4$ as the most probable number of genetic clusters, with the following populations

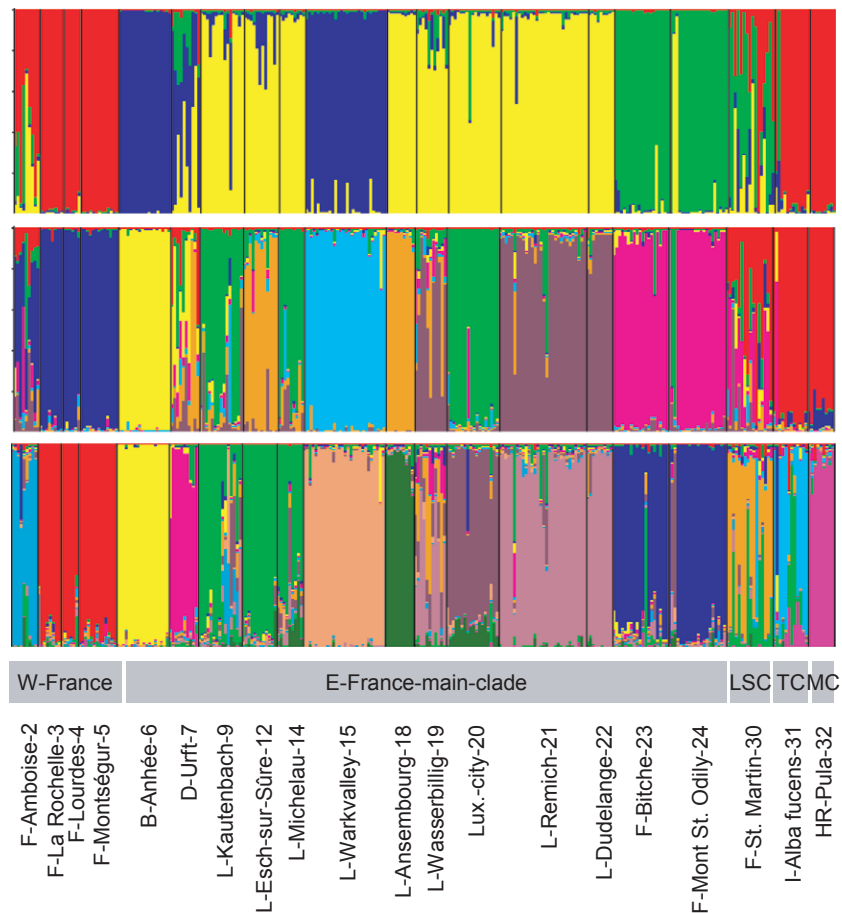
(Fig. 5): (1) Belgium and Germany (6, 7); (2) northern Luxembourg (9–15); (3) southern Luxembourg (18–22); (4) Alsace-Lorraine (23, 24).

Hierarchical ANOVA revealed strong genetic differentiation among the four clades (western France clade, eastern France clade, Tuscany clade and Marche clade; $R_{CT} = 0.769$, $P < 0.0001$). The genetic variance between the western and eastern France clades was also significant ($R_{CT} = 0.314$, $P < 0.0001$). Further AMOVAs were calculated based on the genetic clusters derived from STRUCTURE (Table 3). Very strong genetic differentiation was found even at the regional level, as shown from the genetic variance detected among the three clusters within Luxembourg ($R_{CT} = 0.236$, $P < 0.001$). Genetic distances among populations showed no significant correlation with the geographical distance (Mantel test, $P > 0.05$), but with geographical latitude: pairwise R_{ST} values divided by geographical distances among the respective populations (to obtain a relative value independent of geographical distances) showed a significant correlation between geographical latitude and genetic distances among populations ($r = 0.68$; $P < 0.001$).

Species distribution models

We received a reasonable discriminatory performance for both SDMs (average test AUCs: MAXENT = 0.78;

Figure 4 Results of the Bayesian structure analyses of *Podarcis muralis* populations across Europe, calculated with the program STRUCTURE. Results are shown for $K = 4$ (top), $K = 8$ (highest ΔK ; centre) and $K = 14$ (most probable number of population clusters obtained from GENELAND; bottom). Respective population assignments to mtDNA lineages are shown at the bottom. LSC, Languedoc subclade; TC, Tuscany clade; MC, Marche clade.



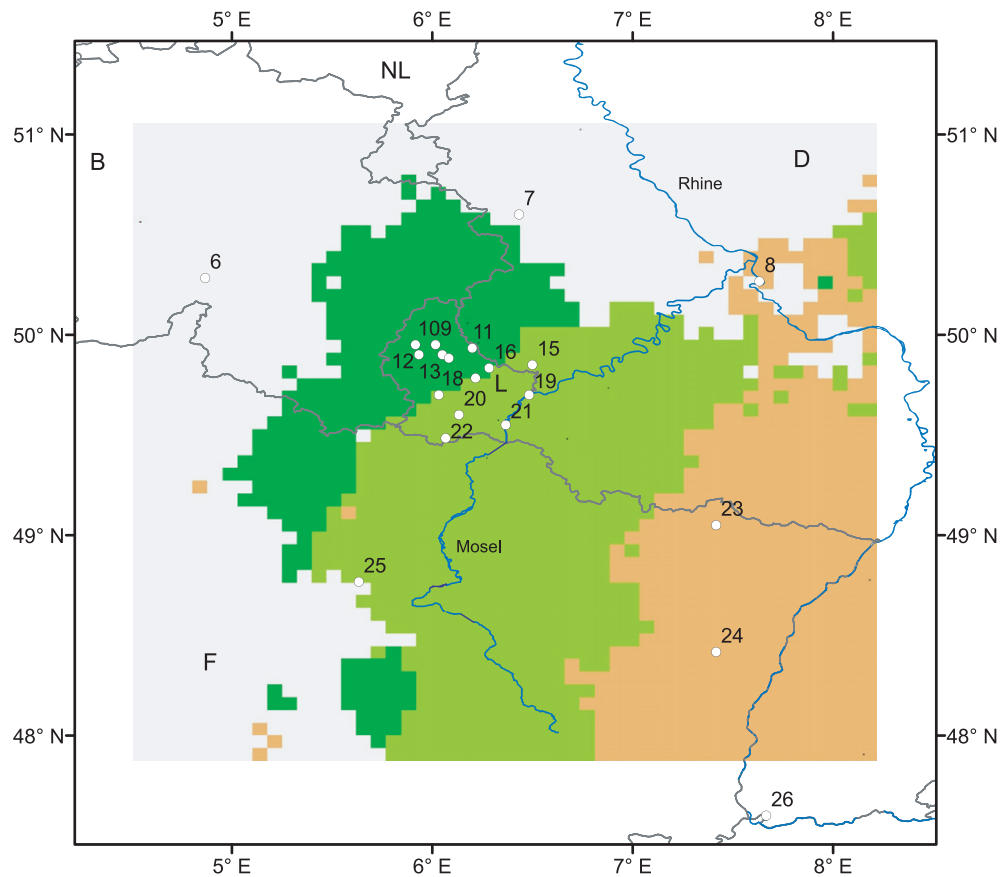


Figure 5 Map of the most probable population membership obtained from GENELAND analysis based on 10 polymorphic microsatellite loci for 13 populations of *Podarcis muralis* located at its northern range margin (including populations 6, 7, 9, 12, 14, 15 and 18–24, coinciding with Table 1). Calculations were performed for $K = 4$. Different colours represent four genetic groups assigning the populations into a north-western cluster (Belgium with Germany) (white), north Luxembourg cluster (dark green), south Luxembourg cluster (light green) and a north-eastern France cluster (light brown). The white dots with numbers represent sampling locations; given numbers coincide with Table 1. B, Belgium; D, Germany; F, France; L, Luxembourg; NL, Netherlands.

Table 3 Hierarchical analyses of molecular variance (AMOVA) testing for significance and degree of genetic differentiation in *Podarcis muralis* in Europe based on 10 polymorphic microsatellites. Variance values (top line) with the respective R statistics (in parentheses). Groupings were created according to the results from the phylogeny of the mtDNA (cytochrome *b*) sequences (^a) and STRUCTURE analyses (^b). ***, $P < 0.0001$; **, $P < 0.001$; *, $P < 0.05$.

Group(s)	Among groups or species (R_{CT})	Among populations within groups (R_{SC})	Within individuals
Four clades ^a	4380.91 (0.7691***)	280.50 (0.2132***)	783.79
Western versus eastern France clade ^a	286.03 (0.3135***)	313.29 (0.500***)	281.93
Two groups ^b	411.61 (0.3784***)	420.11 (0.6195***)	196.01
Four groups ^b	97.35 (0.1166*)	486.97 (0.6534***)	196.01
Eight groups ^b	486.77 (0.5651**)	116.15 (0.3099***)	196.01

BIOCLIM = 0.63), given that the species is a widespread generalist. Across the 10 MAXENT replicates, BIO17 had the highest explanatory power (28.3%), followed by BIO4 (18.1%) and BIO10 (11.1%). Both SDMs correctly identified major parts of the species' current realized distribution according to the IUCN Red List (Böhme *et al.*, 2009) (Fig. 6), even including most of the invasive populations (cf. Schulte *et al.*, 2012b). However, BIOCLIM generally predicted

a larger area than MAXENT. Some smaller parts of the range in northern France were not predicted by MAXENT, but were well covered by BIOCLIM.

For 6 ka, MESS analyses identified only very minor parts of Europe characterized by non-analogous climatic conditions in both scenarios compared to the training area of the SDMs. However, these areas were much more extensive for 21 ka assuming CCSM conditions, but not when assuming

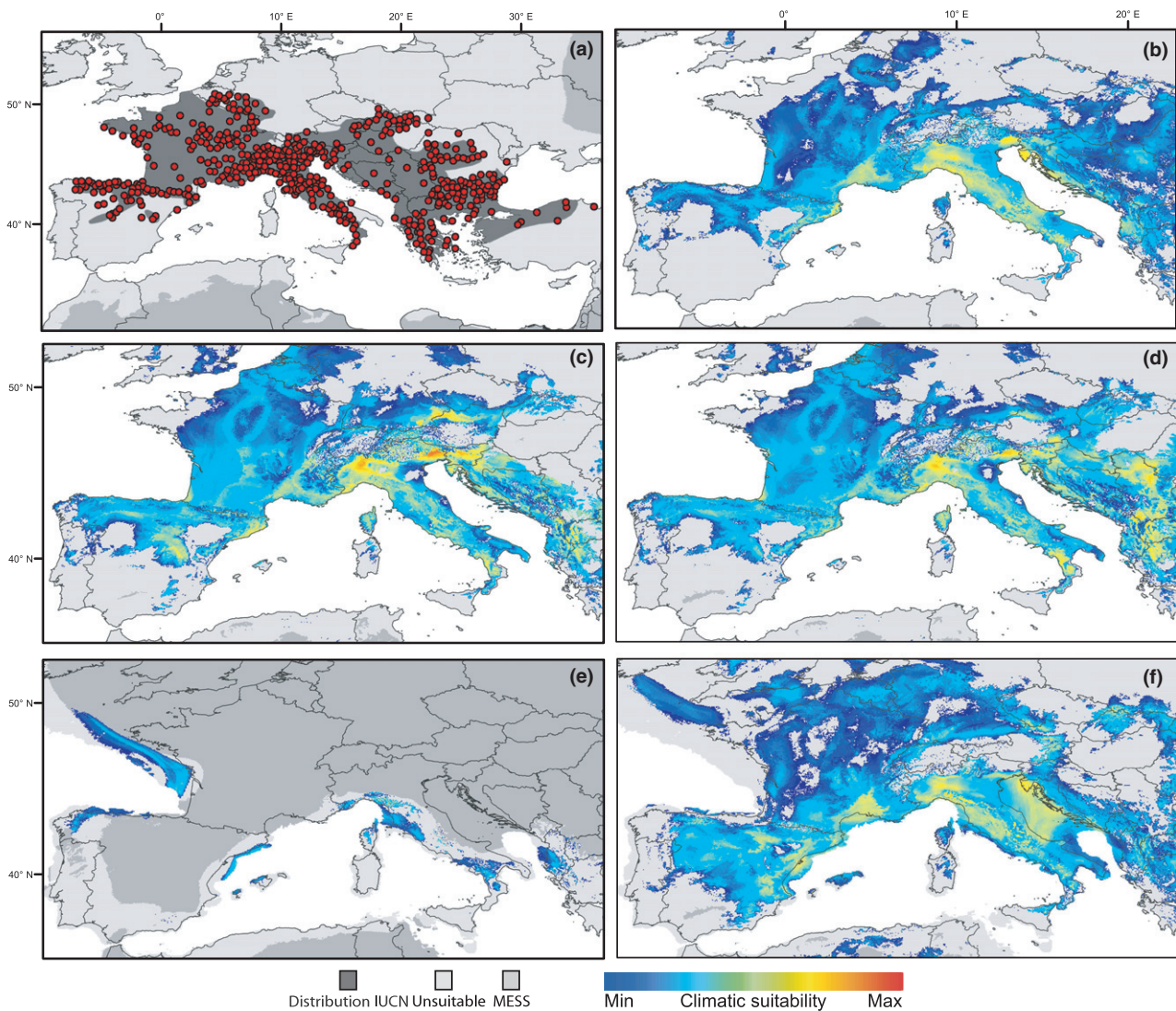


Figure 6 (a) Currently realized distribution of *Podarcis muralis* in Europe (dark shaded area) according to the IUCN Red List (Böhme *et al.*, 2009) and available species records (red dots); (b) the species' current potential distribution derived from a MAXENT species distribution model; (c–f) projections onto two global circulation model scenarios simulating environmental conditions as expected for 6 ka (c, CCSM; d, MIROC) and 21 ka (e, CCSM; f, MIROC). Warmer colours indicate higher climatic suitability. Multivariate environmental similarity surfaces (MESS) identifies those areas with climatic conditions exceeding those of the training region of the SDM making projections less reliable.

those suggested by MIROC. Because all potential refugia are still surrounded by unsuitable climatic conditions, this does not affect the reliability of the SDMs.

DISCUSSION

We identified two major phylogenetic lineages based on *cyt b* mtDNA in Western Europe: the eastern France clade (French Mediterranean coast to Germany, Belgium and Luxembourg) and the western France clade (Pyrenees to Brittany). Within these two clades, a strong nestedness and reduction of allelic diversity and an increase in population genetic differentiation from south to north occurred. Strong intraspecific differenti-

ation was further detected at the landscape level, especially at the northern range margin.

Potential Pleistocene glacial refugia

Our phylogenetic analyses revealed nine distinct genetic clades. These results are concordant with other phylogenetic analyses of *P. muralis* (Giovannotti *et al.*, 2010; Bellati *et al.*, 2011; Schulte *et al.*, 2012a,b,c). While the western France clade shows a rather homogeneous genetic structure for both *cyt b* and microsatellites, the eastern France clade was split into the eastern France main clade and the Languedoc sub-clade, and into various microsatellite clusters (see Fig. 6).

Most thermophilic species (such as *P. muralis*) went extinct in major parts of Central Europe during the late glacial phases and survived at their southern range margin, the southern European peninsulas (Habel *et al.*, 2010). Long-term persistence in these refugia caused distinct evolutionary processes and led to the differentiation of new genetic lineages (Hewitt, 1996, 2001). Our molecular analyses suggest that the differentiation of phylogenetic lineages of *P. muralis* took place during the Pleistocene (Fig. 3), and that the species originated in Calabria, from where it dispersed and formed several new lineages. Differentiation occurred in various refugia. The latest split divided the eastern France main clade from the Languedoc subclade *c.* 380 ka, corresponding to the Elsterian glaciation. The existence of several distinct lineages in Italy (Tuscany, Venetian, Marche, Romagna and Calabria) are in congruence with other biogeographical studies (Giovannotti *et al.*, 2010), and suggests the existence of several refugia within Italy. Another major refugium was most probably located close to the Pyrenees. The genetic pattern we obtained matches the potential refugia projected by SDMs. However, outcomes based on CCSM (Fig. 6e) and MIROC (Fig. 6f) show some incongruences: while CCSM highlights the relevance of the Atlantic coast of western France as a potential refugium, MIROC identifies suitable climate for *P. muralis* at the Mediterranean coast during the past glacial period (this latter scenario is in better congruence with our genetic data). Such discrepancies between past potential distributions derived from CCSM and MIROC scenarios have frequently been reported (e.g. Garcia-Porta *et al.*, 2012; Rebelo *et al.*, 2012) and can be attributed to the different assumptions of the global circulation models.

Northward range expansion

During post-glacial range expansion, various genetic patterns of biogeographical relevance can often be observed, such as the loss of genetic diversity during northward range expansion (Hampe & Petit, 2005) and shifts in allele frequencies due to allele surfing, a process in which rare alleles become common at the leading edge due to genetic drift (Nolte, 2011). Elimination of alleles in the wake of colonization processes (e.g. post-glacial range expansions) and subsequent repeated founder effects and bottlenecks are suggested by our data, confirming results obtained from many other species (Habel *et al.*, 2013). We detected a strong nestedness of allele frequencies, with a significant loss of alleles from southern Europe to the northern margin. This loss of genetic diversity was accompanied by strong allele surfing across nearly all loci, e.g. allele 155 of locus B3 occurs exclusively at the northern range margin of the eastern France clade, becoming the most frequent allele in Anhée (58%) and Urft (45%).

Considering the ecology of *P. muralis* at its north-western range margin (Schulte, 2008), it is likely that post-glacial expansion routes of the eastern France clade followed the River Rhône, passed the Burgundy Gate (as shown for other

organisms; Sternberg, 1998; Schmitt *et al.*, 2002), and colonized major parts of Central Europe downstream of the Moselle river, until it reached its current northern range margin (Fig. 1). Populations at the northern range margin might have benefited from Roman settlements in the Moselle region and the increase in viticulture *c.* 2000 years ago (Guillaume & Lanza, 1982). The western France clade may have expanded along the Garonne and Loire rivers and/or along the Atlantic coastline.

Genetic constitution of populations at the northern margin

The lowest genetic diversity but strongest intraspecific differentiation in *P. muralis* was found in populations at its northern range margin. This positive correlation between genetic differentiation and latitude as well as the negative correlation between genetic diversity and latitude, accompanied by strong population differentiation at the landscape level, suggest a limited exchange of individuals among populations, compared to highly mobile taxa (e.g. Exeler *et al.*, 2008). This trend of increasing genetic differentiation and declining genetic diversity at the leading edge of species' distributions confirms theoretical assumptions of genetic processes along colonization routes (Hampe & Petit, 2005).

The population clusters inferred for the northern range margin are probably caused by corridors along river systems and migration barriers such as mountains. While the locations in southern Luxembourg were most probably colonized via the Moselle valley, the populations in central Luxembourg might have followed the Wiltz river system. The populations in the north of Luxembourg might have migrated via the valley of the River Sauer. Such geographically restricted populations located at the northern distribution range margin are subject to strong population fluctuations, reinforcing genetic differentiation (Hochkirch & Damerau, 2009).

ACKNOWLEDGEMENTS

We thank the Natural History Museum Luxembourg (MNHN), the Research Fund of Luxembourg (FNR), the German Academic Exchange Service (DAAD) and the Deutsche Bundesstiftung Umwelt (DBU) for financial support. We thank Ulrike Schülter (Trier, Germany) for valuable advice in the laboratory. We are grateful to Werner Mayer and Silke Schweiger, Fränz Weiss and the late Paul Müller for providing DNA samples and DNA sequences. Finally, we thank three anonymous referees who improved this article significantly by their comments.

REFERENCES

- Almeida-Neto, M. & Ulrich, W. (2011) A straightforward computational approach for measuring nestedness using quantitative matrices. *Environmental Modelling and Software*, **26**, 173–178.

- Almeida-Neto, M., Guimarães, P., Guimarães, P.R., Jr, Loyola, R.D. & Ulrich, W. (2008) A consistent metric for nestedness analysis in ecological systems: reconciling concept and quantification. *Oikos*, **117**, 1227–1239.
- Beaumont, L.J., Hughes, L. & Poulsen, M. (2005) Predicting species distributions: use of climatic parameters in BIOCLIM and its impact on predictions of species' current and future distributions. *Ecological Modelling*, **186**, 250–269.
- Bellati, A., Pellitteri-Rosa, D., Sacchi, R., Nistri, A., Galimberti, A., Casiraghi, M., Fasola, M. & Galeotti, P. (2011) Molecular survey of morphological subspecies reveals new mitochondrial lineages in *Podarcis muralis* (Squamata: Lacertidae) from the Tuscan Archipelago (Italy). *Journal of Zoological Systematics and Evolutionary Research*, **49**, 240–250.
- Böhme, W., Pérez-Mellado, V., Cheylan, M., Nettmann, H.K., Krecsák, L., Sterijovski, B., Schmidt, B., Lymberakis, P., Podloucky, R., Sindaco, R. & Avci, A. (2009) *Podarcis muralis* (Common Wall Lizard). *IUCN Red List of Threatened Species, version 2012.2*. IUCN, Gland, Switzerland. Available at: <http://www.iucnredlist.org/details/61550>.
- Böttcher, R. (2007) Fossile Amphibien und Reptilien in Baden-Württemberg. *Die Amphibien und Reptilien Baden-Württembergs* (ed. by H. Laufer, K. Fritz and P. Sowig), pp. 62–76. Ulmer-Verlag, Stuttgart.
- Boudjemadi, K., Martin, O., Simon, J.-C. & Estoup, A. (1999) Development and cross-species comparison of microsatellite markers in two lizard species, *Lacerta vivipara* and *Podarcis muralis*. *Molecular Ecology*, **8**, 518–520.
- Braconnot, P., Otto-Bliesner, B., Harrison, S. *et al.* (2007) Results of PMP2 coupled simulations of the Mid-Holocene and Last Glacial Maximum – Part 1: experiments and large-scale features. *Climate of the Past*, **3**, 261–277.
- Brown, R.P., Terrasa, B., Pérez-Mellado, V., Castro, J.A., Hoskisson, P.A., Picornell, A. & Ramon, M.M. (2008) Bayesian estimation of post-Messinian divergence times in Balearic Island lizards. *Molecular Phylogenetics and Evolution*, **48**, 350–358.
- Busack, S.D., Lawson, R. & Arjo, W.M. (2005) Mitochondrial DNA, allozymes, morphology and historical biogeography in the *Podarcis vaucheri* (Lacertidae) species complex. *Amphibia-Reptilia*, **26**, 239–256.
- Busby, J.R. (1991) BIOCLIM – a bioclimatic analysis and prediction system. *Nature conservation: cost effective biological surveys and data analysis* (ed. by C.R. Margules and M.P. Austin), pp. 64–68. CSIRO, Melbourne, Australia.
- Carranza, S., Arnold, E.N. & Amat, F. (2004) DNA phylogeny of *Lacerta (Iberolacerta)* and other lacertine lizards (Reptilia: Lacertidae): did competition cause long-term mountain restriction? *Systematics and Biodiversity*, **2**, 57–77.
- Deichsel, G. & Schweiger, S. (2004) Geographic distribution: *Podarcis muralis*. *Herpetological Review*, **35**, 289–290.
- Drummond, A.J. & Rambaut, A. (2007) BEAST: Bayesian evolutionary analysis by sampling trees. *BMC Evolutionary Biology*, **7**, 214.
- Eckert, C.G., Samis, K.E. & Loughheed, S.C. (2008) Genetic variation across species' geographical ranges: the central–marginal hypothesis and beyond. *Molecular Ecology*, **17**, 1170–1188.
- Elith, J., Graham, C.H., Anderson, R.P. *et al.* (2006) Novel methods improve prediction of species' distributions from occurrence data. *Ecography*, **29**, 129–151.
- Elith, J., Kearney, M. & Phillips, S. (2010) The art of modelling range-shifting species. *Methods in Ecology and Evolution*, **1**, 330–342.
- Elith, J., Phillips, S.J., Hastie, T., Dudík, M., Chee, Y.E. & Yates, C.J. (2011) A statistical explanation of MaxEnt for ecologists. *Diversity and Distributions*, **17**, 43–57.
- Evanno, G., Regnaut, S. & Goudet, J. (2005) Detecting the number of clusters of individuals using the software STRUCTURE: a simulation study. *Molecular Ecology*, **14**, 2611–2620.
- Excoffier, L., Laval, G. & Schneider, S. (2005) Arlequin version 3.0: an integrated software package for population genetics data analysis. *Evolutionary Bioinformatics Online*, **1**, 47–50.
- Exeler, N., Kratochwil, A. & Hochkirch, A. (2008) Strong genetic exchange among populations of a specialist bee, *Andrena vaga* (Hymenoptera: Andrenidae). *Conservation Genetics*, **9**, 1233–1241.
- García-Porta, J., Litvinchuk, S.N., Crochet, P.A., Romano, A., Geniez, P.H., Lo-Valvo, M., Lymberakis, P. & Carranza, S. (2012) Molecular phylogenetics and historical biogeography of the west-palaearctic common toads (*Bufo bufo* species complex). *Molecular Phylogenetics and Evolution*, **63**, 113–130.
- Giovannotti, M., Nisi-Cerioni, P. & Caputo, V. (2010) Mitochondrial DNA sequence analysis reveals multiple Pleistocene glacial refugia for *Podarcis muralis* (Laurenti, 1768) in the Italian Peninsula. *Italian Journal of Zoology*, **77**, 277–288.
- Gómez, A. & Lunt, D.H. (2007) Refugia within refugia: patterns of phylogeographic concordance in the Iberian Peninsula. *Phylogeography of southern European refugia* (ed. by S. Weiss and N. Ferrand), pp. 155–188. Springer, Dordrecht.
- Gotelli, N.J. (2000) Null model analysis of species co-occurrence patterns. *Ecology*, **81**, 2606–2621.
- Gotelli, N.J. & Ulrich, W. (2012) Statistical challenges in null model analysis. *Oikos*, **121**, 171–180.
- Goudet, J. (1995) FSTAT (version 1.2): a computer program to calculate F-statistics. *Heredity*, **86**, 485–486.
- Gruschwitz, M. & Böhme, W. (1986) *Podarcis muralis* (Laurenti 1768) Mauereidechse. *Handbuch der Amphibien und Reptilien Europas, Vol. 2/II, Echsen III* (Podarcis) (ed. by W. Böhme), pp. 155–208. Aula Verlag, Wiesbaden.
- Guillaume, C.-P. & Lanza, B. (1982) Comparaison électrophorétique de quelques espèces de Lacertidés Méditerranéens, Genera *Podarcis* et »*Archaeolacerta*«. *Amphibia-Reptilia*, **3**, 361–375.

- Guillot, G., Mortier, F. & Estoup, A. (2005) GENELAND: a computer package for landscape genetics. *Molecular Ecology Notes*, **5**, 712–715.
- Habel, J.C., Drees, C., Schmitt, T. & Assmann, T. (2010) Refugial areas and postglacial colonizations in the Western Palearctic. *Relict species: phylogeography and conservation biology* (ed. by J.C. Habel and T. Assmann), pp. 189–197. Springer, Dordrecht.
- Habel, J.C., Ulrich, W. & Assmann, T. (2013) Allele elimination recalculated: nested subsets analyses for molecular biogeographical data. *Journal of Biogeography*, **40**, 769–777.
- Hampe, A. & Petit, R.J. (2005) Conserving biodiversity under climate change: the rear edge matters. *Ecology Letters*, **8**, 461–467.
- Harris, D.J., Carranza, S., Arnold, E.N., Pinho, C. & Ferrand, N. (2002) Complex biogeographical distribution of genetic variation within *Podarcis* wall lizards across the Strait of Gibraltar. *Journal of Biogeography*, **29**, 1257–1262.
- Hasumi, H. & Emori, S. (eds) (2004) *K-1 coupled GCM (MIROC) description*. K-1 Technical Report No. 1. Center for Climate System Research, University of Tokyo, Japan.
- Hausdorf, B. & Hennig, C. (2010) Species delimitation using dominant and codominant multilocus markers. *Systematic Biology*, **59**, 491–503.
- Heikkinen, R.K., Luoto, M., Araújo, M.B., Virkkala, R., Thuiller, W. & Sykes, M.T. (2006) Methods and uncertainties in bioclimatic envelope modeling under climate change. *Progress in Physical Geography*, **30**, 751–777.
- Hewitt, G.M. (1996) Some genetic consequences of ice ages, and their role in divergence and speciation. *Biological Journal of the Linnean Society*, **58**, 247–276.
- Hewitt, G.M. (2000) The genetic legacy of the Quaternary ice ages. *Nature*, **405**, 907–913.
- Hewitt, G.M. (2001) Speciation, hybrid zones and phylogeography – or seeing genes in space and time. *Molecular Ecology*, **10**, 537–549.
- Hijmans, R.J., Cameron, S.E., Parra, J.L., Jones, P.G. & Jarvis, A. (2005) Very high resolution interpolated climate surfaces for global land areas. *International Journal of Climatology*, **25**, 1965–1978.
- Hochkirch, A. & Damerau, M. (2009) Rapid range expansion of a wing-dimorphic bush-cricket after the 2003 climatic anomaly. *Biological Journal of the Linnean Society*, **97**, 118–127.
- Huelsenbeck, J.P. & Andolfatto, P. (2007) Inference of population structure under a Dirichlet process model. *Genetics*, **175**, 1787–1802.
- Huelsenbeck, J.P. & Ronquist, F. (2001) MRBAYES: Bayesian inference of phylogenetic trees. *Bioinformatics*, **17**, 754–755.
- Huelsenbeck, J.P., Andolfatto, P. & Huelsenbeck, E.T. (2011) Structurama: Bayesian inference of population structure. *Evolutionary Bioinformatics*, **7**, 55–59.
- Librado, P. & Rozas, J. (2009) DnaSP v5: a software for comprehensive analysis of DNA polymorphism data. *Bioinformatics*, **25**, 1451–1452.
- Nembrini, M. & Oppliger, A. (2003) Characterization of microsatellite loci in the wall lizard *Podarcis muralis* (Sauria: Lacertidae). *Molecular Ecology Notes*, **3**, 123–124.
- Nolte, A.W. (2011) Dispersal in the course of an invasion. *Molecular Ecology*, **20**, 1803–1804.
- Nylander, J.A.A. (2004) *MrModeltest v2*. Program distributed by the author. Evolutionary Biology Centre, Uppsala University, Uppsala, Sweden.
- van Oosterhout, C., Hutchinson, W.F., Wills, D.P.M. & Shipley, P. (2004) MICRO-CHECKER: software for identifying and correcting genotyping errors in microsatellite data. *Molecular Ecology Notes*, **4**, 535–538.
- Otto-Bliesner, B.L., Brady, E.C., Clauzet, G., Tomas, R., Levis, S. & Kothavala, Z. (2006) Last Glacial Maximum and Holocene climate in CCSM3. *Journal of Climate*, **19**, 2526–2544.
- Peterson, A.T. & Nyári, Á.S. (2008) Ecological niche conservatism and Pleistocene refugia in the thrush-like mourner, *Schiffornis* sp., in the Neotropics. *Evolution*, **62**, 173–183.
- Phillips, S.J. & Dudík, M. (2008) Modeling of species distributions with Maxent: new extensions and a comprehensive evaluation. *Ecography*, **31**, 161–175.
- Phillips, S.J., Anderson, R.P. & Schapire, R.E. (2006) Maximum entropy modeling of species geographic distributions. *Ecological Modelling*, **190**, 231–259.
- Podnar, M., Mayer, W. & Tvrtković, N. (2004) Mitochondrial phylogeography of the Dalmatian wall lizard, *Podarcis melisellensis* (Lacertidae). *Organisms Diversity and Evolution*, **4**, 307–317.
- Podnar, M., Mayer, W. & Tvrtković, N. (2005) Phylogeography of the Italian wall lizard, *Podarcis sicula*, as revealed by mitochondrial DNA sequences. *Molecular Ecology*, **14**, 575–588.
- Podnar, M., Haring, E., Pinsker, W. & Mayer, W. (2007) Unusual origin of a nuclear pseudogene in the Italian wall lizard: intergenomic and interspecific transfer of a large section of the mitochondrial genome in the genus *Podarcis* (Lacertidae). *Journal of Molecular Evolution*, **64**, 308–320.
- Poulakakis, N., Lymberakis, P., Antoniou, A., Chalkia, D., Zouros, E., Mylonas, M. & Valakos, E. (2003) Molecular phylogeny and biogeography of the wall-lizard *Podarcis erhardii* (Squamata: Lacertidae). *Molecular Phylogenetics and Evolution*, **28**, 38–46.
- Poulakakis, N., Lymberakis, P., Valakos, E., Pafilis, P., Zouros, E. & Mylonas, M. (2005) Phylogeography of Balkan wall lizard (*Podarcis taurica*) and its relatives inferred from mitochondrial DNA sequences. *Molecular Ecology*, **14**, 2433–2443.
- Pritchard, J.K., Stephens, M. & Donnelly, P. (2000) Inference of population structure using multilocus genotype data. *Genetics*, **155**, 945–959.
- R Development Core Team (2012) *R: a language and environment for statistical computing*. R Foundation for Statistical Computing, Vienna.
- Rambaut, A. (2011) *FigTree 1.3.1*. Available at: <http://tree.bio.ed.ac.uk/software/figtree>.

- Rambaut, A. & Drummond, A. J. (2009) *Tracer v. 1.5*. Available at: <http://beast.bio.ed.ac.uk/Tracer>.
- Rebelo, H., Froufe, E., Brito, J.C., Russo, D., Cistrone, L., Ferrand, N. & Jones, G. (2012) Postglacial colonization of Europe by the barbastelle bat: agreement between molecular data and past predictive modelling. *Molecular Ecology*, **21**, 2761–2774.
- Saavedra, S., Stouffer, D.B., Uzzi, B. & Bascompte, J. (2011) Strong contributors to network persistence are the most vulnerable to extinction. *Nature*, **478**, 233–235.
- Schmitt, T., Gießl, A. & Seitz, A. (2002) Postglacial colonisation of western Central Europe by *Polyommatus coridon* (Poda 1761) (Lepidoptera: Lycaenidae): evidence from population genetics. *Heredity*, **88**, 26–34.
- Schulte, U. (2008) *Die Mauereidechse: erfolgreich im Schlepptau des Menschen*. Laurenti, Bielefeld.
- Schulte, U., Thiesmeier, B., Mayer, W. & Schweiger, S. (2008) Allochthone Vorkommen der Mauereidechse (*Podarcis muralis*) in Deutschland. *Zeitschrift für Feldherpetologie*, **15**, 139–156.
- Schulte, U., Gassert, F., Geniez, P., Veith, M. & Hochkirch, A. (2012a) Origin and genetic diversity of an introduced wall lizard population and its cryptic congener. *Amphibia-Reptilia*, **33**, 129–140.
- Schulte, U., Hochkirch, A., Lötters, S., Rödder, D., Schweiger, S., Weimann, T. & Veith, M. (2012b) Cryptic niche conservatism among evolutionary lineages of an invasive lizard. *Global Ecology and Biogeography*, **21**, 198–211.
- Schulte, U., Veith, M. & Hochkirch, A. (2012c) Rapid genetic assimilation of native wall lizard populations (*Podarcis muralis*) through extensive hybridization with introduced lineages. *Molecular Ecology*, **21**, 4313–4326.
- Selkoe, K.A. & Toonen, R.J. (2006) Microsatellites for ecologists: a practical guide to using and evaluating microsatellite markers. *Ecology Letters*, **9**, 615–629.
- Sommer, R.S. & Zachos, F.E. (2009) Fossil evidence and phylogeography of temperate species: ‘glacial refugia’ and post-glacial recolonization. *Journal of Biogeography*, **36**, 2013–2020.
- Sternberg, K. (1998) The postglacial colonization of Central Europe by dragonflies, with special reference to southwestern Germany (Insecta, Odonata). *Journal of Biogeography*, **25**, 319–337.
- Stone, L. & Roberts, A. (1992) Competitive exclusion, or species aggregation? An aid in deciding. *Oecologia*, **91**, 419–424.
- Swets, J.A. (1988) Measuring the accuracy of diagnostic systems. *Science*, **240**, 1285–1293.
- Ulrich, W. & Gotelli, N.J. (2013) Pattern detection in null model analysis. *Oikos*, **122**, 2–18.
- Yu, Y., Harris, A.J. & He, X.-J. (2010) S-DIVA (statistical dispersal–vicariance analysis): a tool for inferring biogeographic histories. *Molecular Phylogenetics and Evolution*, **56**, 848–850.
- Yu, Y., Harris, A.J. & He, X.J. (2011) RASP (*Reconstruct Ancestral State in Phylogenies*) 2.0b. Available at: <http://mnh.scu.edu.cn/soft/blog/RASP>.

SUPPORTING INFORMATION

Additional Supporting Information may be found in the online version of this article:

Appendix S1 Overview of all cytochrome *b* sequence data used in our study.

Appendix S2 Results obtained from the program RASP.

Appendix S3 Estimates of cluster number (*K*) from STRUCTURE and STRUCTURAMA analyses using ten microsatellite loci for *K* = 1–20 (individuals) of *Podarcis muralis*.

BIOSKETCH

Franz Gassert studied biogeography at the University of Saarbrücken (Germany) and undertook his PhD in the field of population genetics and phylogeography at Trier University working on the biogeography of the common wall lizard, *Podarcis muralis*. He is currently working on various research projects in the field of population genetics at the Department of Behavioural Genetics, Trier University, Germany.

Author contributions: F.G., E.E., A.H. and J.C.H. conceived the ideas; F.G. collected and analysed the data; all authors wrote the manuscript and aided in the interpretation of the data.

Editor: Aristeidis Parmakelis